



# High sensitive and selective flexible H<sub>2</sub>S gas sensors based on Cu nanoparticle decorated SWCNTs



Mohsen Asad <sup>a,\*</sup>, Mohammad Hossein Sheikhi <sup>a</sup>, Mahdi Pourfath <sup>b,c</sup>, Mahmood Moradi <sup>d</sup>

<sup>a</sup> School of electrical and computer engineering, Shiraz University, 71345-1585 Shiraz, Iran

<sup>b</sup> School of Electrical and Computer Engineering, University of Tehran, 14395-515 Tehran, Iran

<sup>c</sup> Institute for Microelectronics, TU Wien, Gusshausstrasse 27-29/E360, 1040 Vienna, Austria

<sup>d</sup> Department of Physics, Shiraz University, 71345-1585 Shiraz, Iran

## ARTICLE INFO

### Article history:

Received 11 August 2014

Received in revised form

24 November 2014

Accepted 20 December 2014

Available online 27 December 2014

### Keywords:

Carbon nanotubes

Copper nanoparticles

Flexible sensors

Polyethylene terephthalate

H<sub>2</sub>S sensing

## ABSTRACT

We present sensitive flexible H<sub>2</sub>S gas sensors operating at room temperature based on Cu-SWCNTs. SWCNTs are decorated with metallic cluster of Cu nanoparticles (NPs) by employing a reduction chemical process and are spin coated on a polyethylene terephthalate (PET) flexible substrate for achieving facile and cheap sensors. Cu-SWCNTs-based sensors show remarkable responses upon exposure to various concentrations of H<sub>2</sub>S gas in the range of 5 ppm to 150 ppm. A fast response time and a recovery time of ~10 s and ~15 s, respectively, are obtained for 5 ppm of H<sub>2</sub>S. Resistance modulation – without any significant degradation – is observed for bending radii larger than 4 mm. The sensors show reproducible response upon exposure to larger than 20 ppm of H<sub>2</sub>S and bending radii larger than 7.8 mm. Ab initio simulations are performed to explore the underlying H<sub>2</sub>S sensing mechanism of Cu-SWCNTs. In agreement with our experiments, theoretical analyses indicated that the decoration of SWCNTs with Cu atoms enhances the sensitivity of SWCNTs for H<sub>2</sub>S gas detection.

© 2014 Elsevier B.V. All rights reserved.

## 1. Introduction

Recently, intense research efforts have been dedicated to the development of detectors and sensors for detecting ultra-low amounts of chemical agents with a relatively fast response time [1,2]. H<sub>2</sub>S is a harmful gas to human that can cause death depending on the concentration and exposure time [3]. Hydrogen sulfide has serious erosion effects and is known to be the major source of acid rain. Hydrogen sulfide is generated in various industrial processes including natural gas processing and petroleum refining. Although several commercial devices have been developed for H<sub>2</sub>S monitoring, they suffer from high operating temperatures, high power consumption, and high cost [4–6]. Harmful effects of H<sub>2</sub>S, however, require the development of small, portable, fast, and sensitive gas sensors.

A single wall carbon nanotube (SWCNT) can be considered as a graphene sheet that has been rolled up into a seamless nanocylinder [7]. CNTs are being used as building blocks of advanced functional materials due to their excellent electrical properties

[8–10]. SWCNTs have been widely used as the channel materials for field effect transistors (FETs) [11–13], electrochemical sensors [14–17], gas sensors [18–22], and biosensors [23–25]. The sensitivity of CNTs to the surface charge transfer is the key advantage of their applications as sensing elements [26]. Because of low level selectivity and sensitivity of pristine SWCNTs to chemical gases, various approaches have been used for functionalizing SWCNTs by polymers [27], enzymes [28] and metallic clusters [29].

In recent years, flexible sensors have been extensively used for direct attachment to the body skin for wearable smart and portable consumer device applications [30,31]. Flexible sensors can be adopted for a wide range of applications due to their light weight, low cost, and mechanical flexibility [32–34]. Excellent mechanical properties of CNTs render them as prominent candidates for flexible devices. Recent studies show that CNTs can be easily assembled on flexible substrates using spray and plasma treatments [35]. Therefore, flexible sensors with CNTs are very promising for gas sensing application [36–38]. In this study, we present relatively fast and flexible sensors, employing SWCNTs decorated with Cu NPs for the detection of H<sub>2</sub>S. SWCNTs-based sensors are fabricated on a polyethylene terephthalate (PET) substrate which has a high degree of flexibility and transparency.

\* Corresponding author. Tel.: +98 9127123010.

E-mail address: [mohsenasad@shirazu.ac.ir](mailto:mohsenasad@shirazu.ac.ir) (M. Asad).

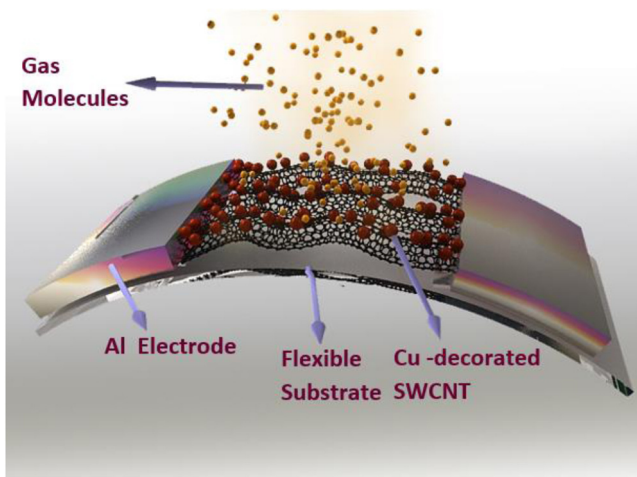


**Fig. 1.** The schematic of the fabricated SWCNT-based gas sensors on a flexible substrate.

## 2. Experiments

### 2.1. Materials and methods

SWCNTs (with outer diameters of  $\sim 1\text{--}2\text{ nm}$ , lengths of  $\sim 30\text{ }\mu\text{m}$ , purity 90%, supplied by Parsis Co. Iran) are used as building blocks of the sensitive film. SWCNTs sidewalls are functionalized by carboxyl groups using acid treatment process: 50 mg of pristine SWCNTs are dispersed in a solution of  $\text{H}_2\text{SO}_4:\text{HNO}_3$  (1:3) followed by sonication at  $60^\circ\text{C}$  for 2 h. This process leads to the formation of active sites that are negatively charged which in turn facilitate chemical bonds. Functionalized SWCNTs (F-SWCNTs) are filtered and washed with DI water several times until a neutral PH is achieved. The F-SWCNTs are decorated by Cu NPs by a chemical reduction process: 50 mg F-SWCNTs are added in DI water and stirred for 15 min. Then 20 mg  $\text{CuSO}_4$  are added in solution consequently and stirred at  $80^\circ\text{C}$  for 30 min. Following this process Cu ions (in the shape of  $\text{Cu}^+$  and  $\text{Cu}^{2+}$ ), as described by Pike et al. [39], are reduced and deposited on the functionalized sites at SWCNT's walls which are negatively charged. The final nanomaterial is filtered and dried in vacuum oven at  $60^\circ\text{C}$  for 8 h.

Aluminum interdigital transducers (IDTs) are used as contacts for Cu decorated SWCNTs (Cu-SWCNTs) based gas sensors. In order to fabricate IDTs on flexible substrates, micro-scale patterning on PET films can be employed: a layer of photoresist is patterned on the substrate with conventional photolithography process, 200 nm of Al layer (deposited by DC magnetron sputtering system, Nanosstructured Coating Co., Iran) is then coated on the substrate followed by a lift-off process by the immersion of the flexible substrate in sonicated acetone. Finally, Cu-SWCNTs are spin-coated onto the patterned substrate and then annealed in a vacuum oven at  $80^\circ\text{C}$  for 30 min. Fig. 1 shows the schematic structure of a flexible sensor with assembled Cu-SWCNTs.

### 2.2. Characterization

The surface morphology of Cu-SWCNTs is characterized using field emission scanning electron microscope (FE-SEM, Hitachi S4160). We have performed Energy Dispersive Spectroscopy (EDS) analysis on the Cu NP decorated SWCNTs to indicate the Cu loading on the final sensitive film. For sensitivity assessing of the fabricated sensors, they are loaded in an aluminum chamber (150 ml volume) and they are outgassed in the vicinity of argon gas for 1 min. Argon is used as a dilution gas for removing the effect of humidity and oxygen on the sensing mechanism of the fabricated sensors. The required concentrations of  $\text{H}_2\text{S}$  and argon are measured by mass

flow controllers. The time dependent electrical resistance is measured at various gas concentrations from 5 ppm to 150 ppm, using a computer-based data acquisition system. For the measurements a fix bias voltage of 1 V is applied to Al electrodes. For the recovering process, after steady state, each sensor is exposed to dry argon to attain 90% of the total resistance change. Before each measurement, the outgassing procedure is carried out by holding the sensors in a constant flow of argon and the initial resistance is registered. To evaluate the selectivity toward various gases, the devices are exposed to acetone, ethanol, and  $\text{H}_2$ . The effects of bending radius on the flexible sensors are analyzed at bending radii larger than 4 mm. Influence of the humid condition on the response characteristics of the fabricated sensors has been investigated under 40% relative humid ambient at room temperature.

### 2.3. Computational method

To understand the adsorption mechanism of  $\text{H}_2\text{S}$  gas in Cu-SWCNTs, ab initio studies are performed, employing the SIESTA code [40]. Two (10,0) carbon chains are selected as the unit cell. The structure of the isolated (10,0) SWCNT, Cu-SWCNT,  $\text{H}_2\text{S}$  and their complex system ( $\text{H}_2\text{S}/\text{Cu-SWCNTs}$ ) are optimized by GGA pseudo potential approximation. To optimize the geometry of the atoms, the minimum force on each atom is set to  $0.05\text{ eV}/\text{\AA}$ . The mesh cut-off energy is set to 150 Ry. An unrestricted  $1 \times 1 \times 4$  Monkhorst-Pack grid for k-point sampling of the Brillouin zone is used [41]. Three different initial configurations of Cu-SWCNTs are considered for the optimization processes. Finally, the adsorption of a single  $\text{H}_2\text{S}$  molecule on the Cu-SWCNTs is considered. One of the main focuses in this calculation is to obtain the binding energies and electronic properties of the Cu-SWCNT due to  $\text{H}_2\text{S}$  gas adsorption. The binding energy of  $\text{H}_2\text{S}$  molecule adsorption on the Cu-SWCNT ( $E_b$ ) is calculated as follows:

$$E_b = E(\text{H}_2\text{S/Cu-SWCNT}) - E(\text{Cu-SWCNT}) - E(\text{H}_2\text{S}), \quad (1)$$

where  $E(\text{H}_2\text{S/Cu-SWCNT})$  is the total energy of the  $\text{H}_2\text{S}$  adsorbed on the Cu-SWCNT,  $E(\text{Cu-SWCNT})$  is the total energy of the Cu-SWCNT, and  $E(\text{H}_2\text{S})$  is the total energy of the isolated  $\text{H}_2\text{S}$  molecule.

## 3. Results and discussions

### 3.1. Structural study and EDS analysis

Fabricated devices on a PET substrate are shown in Fig. 2a. The photograph clearly shows that the substrate with Al electrodes can be easily bent. The electrode fingers have a height of  $5000\text{ }\mu\text{m}$  and a gap size of  $200\text{ }\mu\text{m}$ . Spin coated thin films of Cu-SWCNTs show strong adherence on the substrate. As shown in Fig. 2b pristine SWCNTs are dispersed as bare bundles and Fig. 2c illustrates that SWCNT bundles are successfully decorated with Cu NPs. The dense decoration of Cu NPs on the sidewalls of SWCNTs leads to increased sensitivity of the sensors. Fig. 2c depicts densely linked metallic cluster of Cu nanoparticles on the CNT sidewalls.

The elemental composition of SWCNTs decorated with metallic cluster of Cu NPs has been investigated by EDS analysis. Fig. 2d shows the elemental ratio of Cu, O and C peaks. The oxygen peak can be attributed to functionalized surface of the SWCNT after acid treatment and also to the presence of the CuO composition at the sidewalls of the SWCNT. The qualitative and quantitative analyses have been used to find out what elements in which relativity exists in our prepared sensitive material. The EDS analysis represents the Cu/C peak ratio of 0.25, which is consistent with decomposition of  $\text{CuSO}_4$  and reduction of Cu ions into metallic nanocluster. By adjusting the concentration of  $\text{CuSO}_4$  in the starting solution, the Cu loading in the final Cu-SWCNTs sensitive material can be controlled.

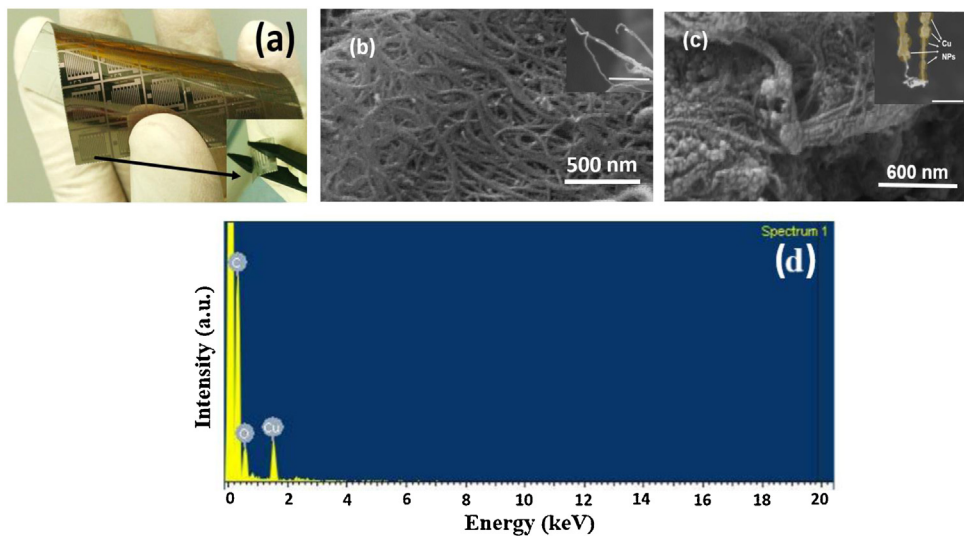


**Fig. 2.** (a) Optical image of the fabricated devices on the flexible substrate. The inset depicts a single device. SEM images of (b) bare SWCNTs after acid treatment (the inset figure scale bar is 600 nm) and (c) after decoration with Cu NPs which shows successful decoration of sidewalls with NP clusters (the inset figure scale bar is 500 nm). (d) EDS analysis of Cu-SWCNTs sensitive material.

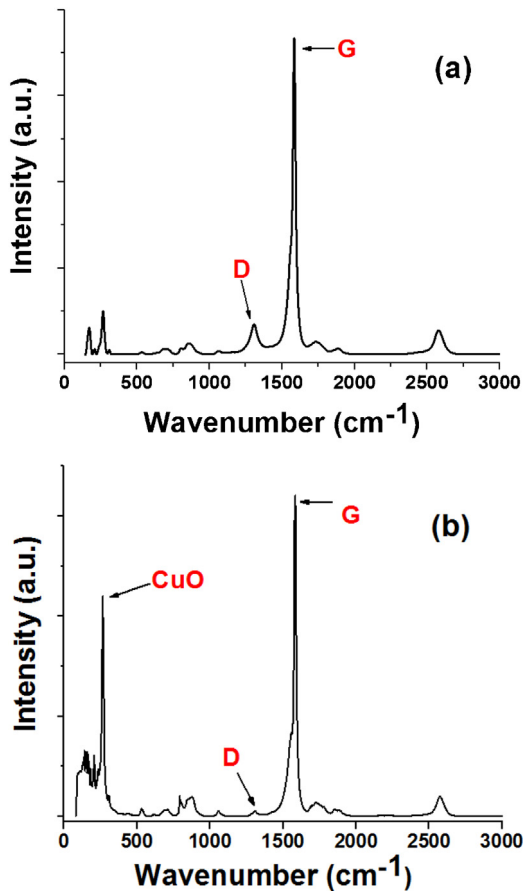


**Fig. 3.** Raman spectra of the (a) SWCNTs after acid treatment and (b) SWCNTs after decoration with Cu NPs.

### 3.2. Raman spectroscopy

Cu-SWCNTs synthesized in this study are also characterized using Raman spectroscopy in order to determine the phase and chemical structures. Fig. 3a shows the distinguished peaks of F-SWCNT are G and D bands that are originating from the Raman

active mode of graphite around  $1582 \text{ cm}^{-1}$  and  $1350 \text{ cm}^{-1}$ , respectively [42]. The G band is attributed to the  $E_{2g}$  phonons of  $\text{sp}^2$  states and the D band is attributed to the  $A_{1g}$  symmetry. In the low frequency region, the spectrum is dominated by the in-phase mode known as radial breathing mode (RBM).

The Raman spectrum of SWCNTs decorated with Cu NPs is shown in Fig. 3b. The spectrum has a strong peak located at around  $300 \text{ cm}^{-1}$  which is assigned to CuO [43]. Our structural result is the same as the one that has been studied by Yin et al. [44] for CuO NPs synthesized by chemical route. The results clearly indicate the successful growth of Cu NPs on SWCNT sidewalls.

In addition, the intensity of the D band brings from the in-plane transverse optical phonon mode. This intensity shows the defect concentration along the tube [42]. Comparing the intensity ratio of D/G bands ( $I_D/I_G$ ) shown in Fig. 3a and b clarifies that after SWCNTs decoration with Cu NPs, the defect concentration decreases which it can be due to chemical bond formation between NPs and defect sites at SWCNTs side walls.

### 3.3. $\text{H}_2\text{S}$ sensing response characteristics

Upon the exposure of the sensors to  $\text{H}_2\text{S}$  gas, the adsorption of the molecules at the surface modulates the conductivity. The sensor response is defined as a relative variation of the resistance:

$$\Delta R(\%) = \frac{R_g - R_0}{R_0} \times 100 \quad (2)$$

where  $R_g$  and  $R_0$  are the resistances of the sensor in the presence and the absence of gas, respectively. The sensor response is evaluated five times and the presented results are the median of all responses. Fig. 4a presents the dynamics of the sensor response at various concentrations of  $\text{H}_2\text{S}$  at room temperature (about  $27^\circ\text{C}$ ). The results show that, these sensors capable of detecting  $\text{H}_2\text{S}$  as low as 5 ppm. The response time and the recovery time are about 10 s and 15 s, respectively, for 5 ppm of  $\text{H}_2\text{S}$ .

Zhang et al. [45] have previously reported that for pristine SWCNTs, there is no interaction with  $\text{H}_2\text{S}$  as a target gas. The observed resistance modulation of our sensors is related to the presence of metallic nanoparticles. The adsorbed  $\text{H}_2\text{S}$  molecule can be split into

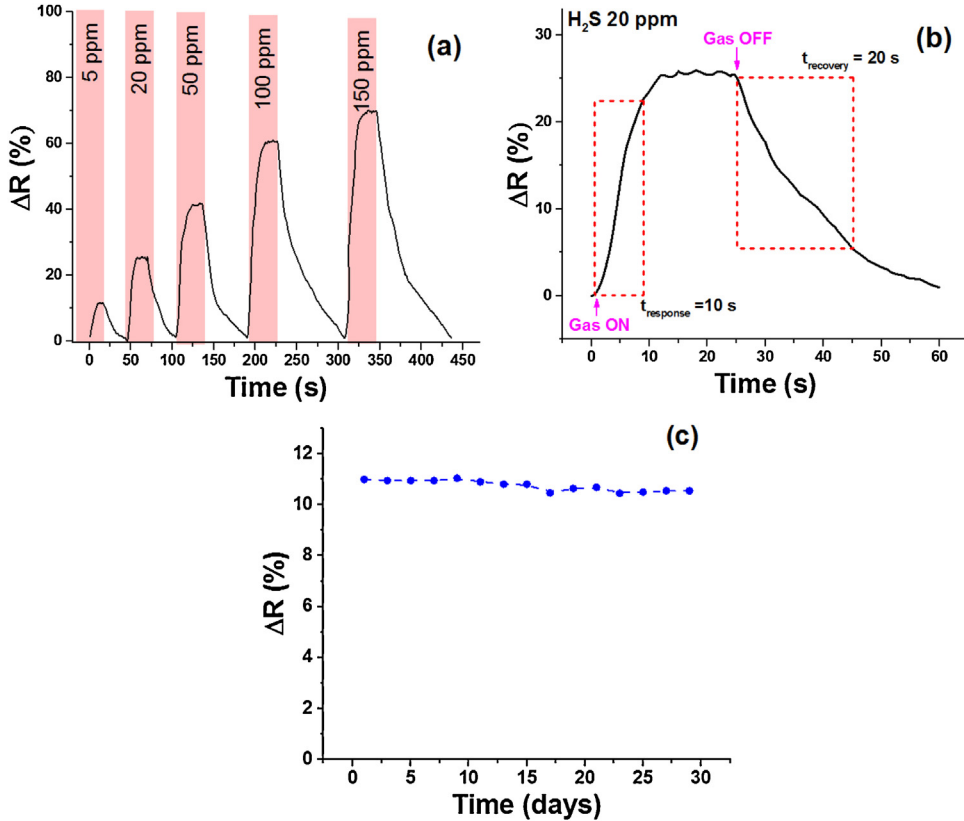


**Fig. 4.** (a) Sensor response to various H<sub>2</sub>S gas concentrations at room temperature. (b) Enlarged response curve of the sensor under exposing to 20 ppm H<sub>2</sub>S (c) Long-term evaluation of the sensor's response to 5 ppm H<sub>2</sub>S gas at room temperature.

sulfur adatom and hydrogen ions due to catalytic properties of Cu NPs:



The cleavage of H<sub>2</sub> from H<sub>2</sub>S in the vicinity of a SWCNT leads to the breakdown of H<sub>2</sub> into H<sup>+</sup> ions and giving electrons to the SWCNT [46]:



This chemical process leads to the resistance modulation of the sensitive films.

Fig. 4b presents the enlarged part of the measured response curve to 20 ppm of the Cu-SWCNTs based sensors. It is seen from the figure that, the resistance increased rapidly when the sensors were exposed to 20 ppm H<sub>2</sub>S. As well as fast response time, the recovery time was measured to be 20 s while the resistance recovered to 10% of the final response value when the H<sub>2</sub>S was purged from the chamber and argon was introduced.

Fig. 4c shows a plot of the one sensor's response upon exposure to 5 ppm H<sub>2</sub>S during a period of 30 days. Each measurement was performed every 2 days after 30 min purging process under argon ambient and the response of the sensor monitored under exposure to H<sub>2</sub>S gas. This process helped us to remove any moisture content which might accumulated in the interior of the chamber. After 17 day, a slight decrease in the response was observed. This deviation was probably due to unwanted impurities on the surface of the Cu-SWCNTs sensitive film which were not desorbed at room temperature. The long-term evaluation of the Cu-SWCNTs based flexible sensor reveals that the H<sub>2</sub>S sensing performance of the sensors was kept almost the same as initial measurement.

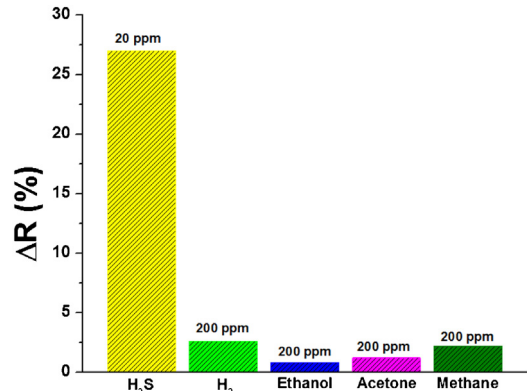


**Fig. 5.** The selectivity of the fabricated sensors to various gases. The H<sub>2</sub>S concentration is kept at 20 ppm while the concentrations of other interfering gases are fixed at 200 ppm.

### 3.4. Selectivity evaluation

The optimized sensors must be insensitive to other interfering environmental gases. The response of the fabricated sensors is measured toward various interfering gases including H<sub>2</sub>, acetone, ethanol and methane in 200 ppm concentration at room temperature. Although the concentration of H<sub>2</sub>S was fixed at 20 ppm, the fabricated sensors are highly selective to H<sub>2</sub>S compared to the other interfering gases, see Fig. 5. The very low tendency of the sensors toward H<sub>2</sub> and methane can be also attributed to liking splitting of the hydrogen ions from their molecules in the vicinity of the catalytic Cu NPs.

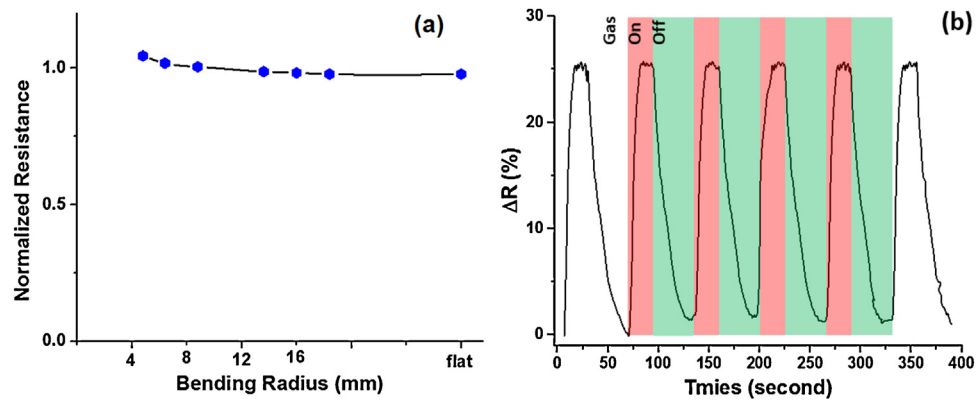


**Fig. 6.** (a) normalized resistance of the Cu-SWCNTs-based flexible devices as a function of the bending radius and (b) the sensor response upon exposure to 20 ppm  $\text{H}_2\text{S}$  gas and a bending radius of 7.8 mm.

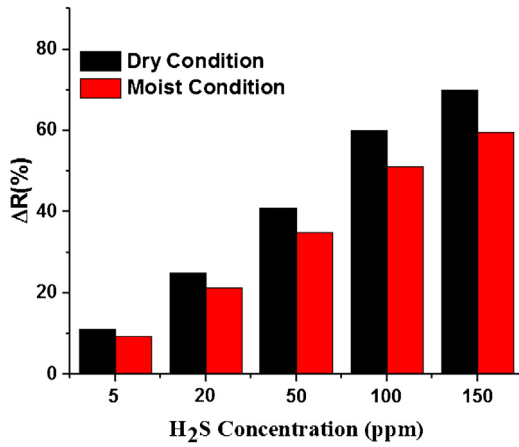


**Fig. 7.** Final response of the Cu-SWCNTs based flexible sensor under 40% relative humidity and dry environment at room temperature.

### 3.5. Effect of sensor bending on the gas sensing properties

In order to evaluate the stability of the sensor response, a bending test is performed and the chemiresistive sensor characteristics are measured as a function of the bending radius, see Fig. 6a. After bending of flexible sensors 10 times, no significant degradation is observed which shows the quality and stability of the film for flexible application. Fig. 6b presents the reproducibility and stability of the sensor response in the presence of 20 ppm  $\text{H}_2\text{S}$  and a bending radius of 7.8 mm.

### 3.6. Influence of the moisture on the sensor's response

The influence of the humid condition on the sensing properties of the Cu-SWCNTs based flexible sensors was measured under 40% relative humidity (13,000 ppm) at room temperature. Fig. 7 shows the final response of the sensors at various concentrations of  $\text{H}_2\text{S}$  gas under moist and dry conditions. For assuring on the obtained results, the sensors were kept 10 min in moist  $\text{H}_2\text{S}$  gas before any measurement. The results show that the response sensitivity of the sensor decreased about 15% under moist condition. This indicated that physisorption plays major role in the interaction between water molecules and Cu-SWCNTs sensitive film.

From the above results, it is clear that our fabricated flexible sensors based on the Cu-SWCNTs sensitive film indicate promising sensing response times toward  $\text{H}_2\text{S}$  gas. In present study, enhanced response time of 10 s for 5 ppm  $\text{H}_2\text{S}$  gas has been obtained which shows an improvement in comparison with 15 s for 3 ppm by Kong

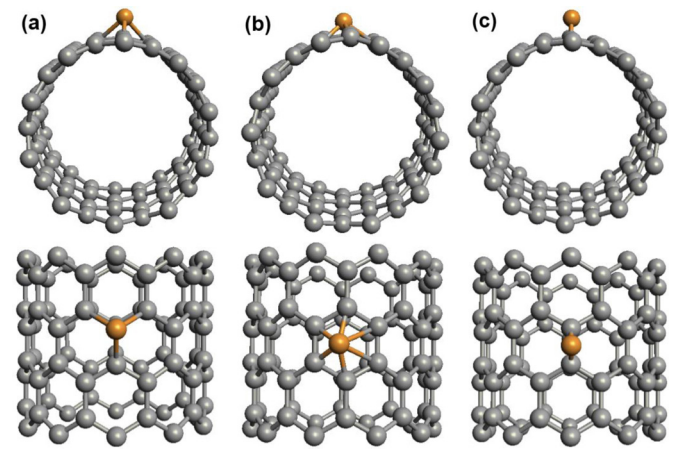


**Fig. 8.** Three possible configurations Cu-SWCNT: (a) directly above a C atom, (b) at the center of hexagon and (c) at the center of a C–C bond (bridge site).

et al. [47], 15 s for 20 ppm by Chowdhuri et al. [48], 15 s for 50 ppm by Wagh et al. [49] and 80 s for 50 ppm by Katti et al. [50]. These fast responses in the Cu based sensitive materials can be explained by the highest catalytic properties of Cu and their oxides toward splitting of  $\text{H}_2\text{S}$  molecules into their adatoms and ions. The recovery time of 15 s under exposing to 5 ppm  $\text{H}_2\text{S}$  shows a significant improvement in comparison with 481 s for 20 ppm by Park et al. [51], 415 s for 3 ppm by Kolmakov et al. [52] and 30 s for 10 ppm by Lin et al. [53].

### 3.7. Sensing mechanism

Ab initio simulations are employed to understand the adsorption properties of  $\text{H}_2\text{S}$ . To study the adsorption of a single Cu atom onto a SWCNT surface, we consider various configurations of one Cu atom per two carbon chains of the CNT: at the top site above a C atom, at the center of the hexagon (hollow site), and at the center of a C–C bond (bridge site), see Fig. 8. The optimized structures using GGA method are presented in Fig. 9. After optimization, the binding energy of the Cu-SWCNT is calculated for all mentioned possible configurations. According to the obtained binding energies, the strongest chemical bonding between the Cu atom and the SWCNT takes place in the bridge site configuration (Fig. 9c), whereas the hollow site shows the weakest interaction (Fig. 9b). Hence, the bridge site configuration shows the most stable structure of the Cu-SWCNT which is used for later calculations of  $\text{H}_2\text{S}$  adsorption.

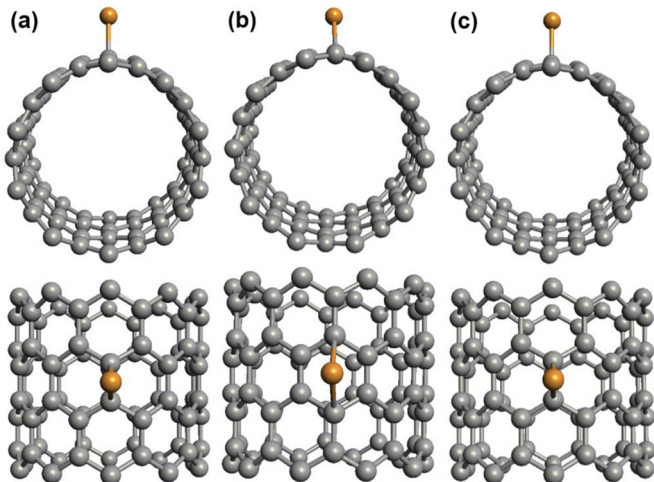


**Fig. 9.** Optimized configurations of Cu-SWCNT. The forces on each atom are being smaller than 0.05 eV/Å and the cutoff energy is 150 Ry.

The most stable adsorption geometry of H<sub>2</sub>S molecule is calculated among from three possible configurations depending on the adjacent H or S atom to the Cu-SWCNT. The results indicate that the most stable configuration is the one in which H<sub>2</sub>S is kept to the Cu-SWCNT surface with S end toward the Cu atom. Fig. 10 demonstrates the primary and the optimized structures for these adsorptions. Therefore, the main chemical interactions in H<sub>2</sub>S/Cu-SWCNT system involve the chemical bonding between Cu and S atoms.

atoms in chorus with devotion of H atoms toward SWCNT consecutively (see Section 3.3). Binding energy calculations indicate the configuration in Fig. 10c has the strongest interaction between the H<sub>2</sub>S molecule and the Cu-SWCNT, compared to other configurations. The magnitude of the binding energy for the most stable H<sub>2</sub>S/Cu-SWCNT is −6.43 eV, which indicates strong chemisorption of H<sub>2</sub>S molecule on the Cu-SWCNT. For binding energies smaller than zero, the energy of the adsorption system is smaller than the isolated Cu-SWCNT and gas molecules. Therefore, in this case the interaction is exothermic and spontaneous.

In case of charge transfer between the H<sub>2</sub>S molecule and the Cu-SWCNT, any changes in electrical properties of the system can be attributed to this charge transfer. Fig. 11 shows the DOS of a pristine (10,0) SWCNT, Cu-SWCNT and H<sub>2</sub>S/Cu-SWCNT system. The results clearly reveal that the Cu decoration modifies the electronic structure of the system, i.e. the Fermi level is raised into the conduction band and the SWCNT becomes electron-rich. The right side of Fig. 11 depicts a closer view of the DOS around the Fermi level. The results indicate that the Fermi level of the H<sub>2</sub>S/Cu-SWCNT system shifts 0.5 eV toward higher energy, in comparison with a pristine SWCNT.

Ab initio simulations indicate that the band gap of the pristine (10,0) SWCNT is 0.694 eV (Fig. 12a). After decoration by Cu atoms, the Fermi level shifts toward the conduction band and the Cu-SWCNT become electron rich. After the adsorption process, the H<sub>2</sub>S/Cu-SWCNT becomes n-type also with more occupied conduction bands in comparison with the Cu-SWCNT system (Fig. 12c). These results validate the chemical interaction presented in Equation 4.

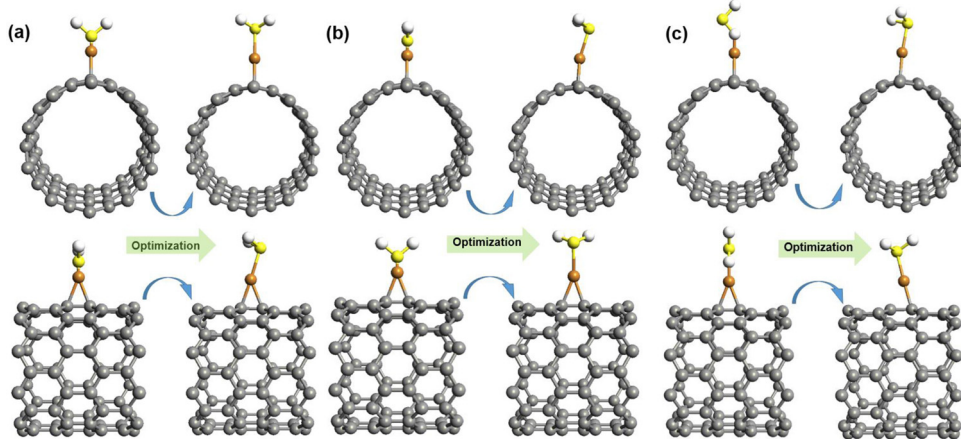


**Fig. 10.** The optimized structures for a single H<sub>2</sub>S molecule adsorbed on a SWCNT with three possible configurations: (a) S atom is the nearest atom to Cu-SWCNT, (b) S atom is the nearest atom to Cu-SWCNT [with 90° rotation of (a)], and (c) the H atom is the nearest atom to Cu-SWCNT.

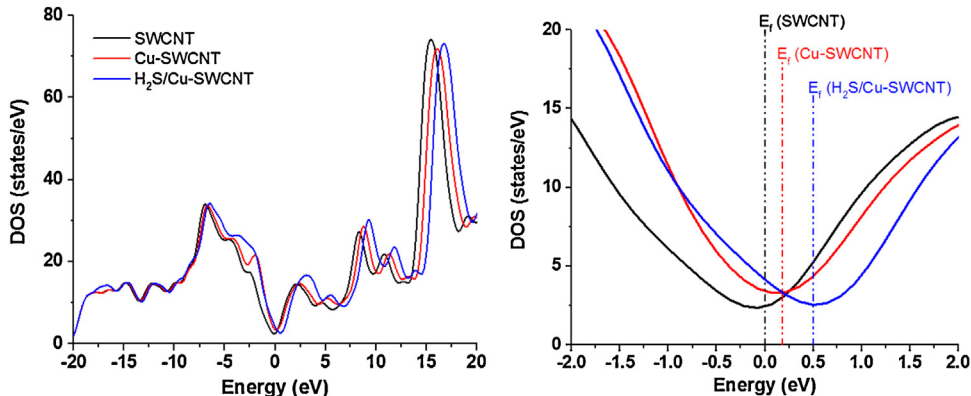


**Fig. 11.** The DOS of SWCNT, Cu-SWCNT, and H<sub>2</sub>S/Cu-SWCNT.

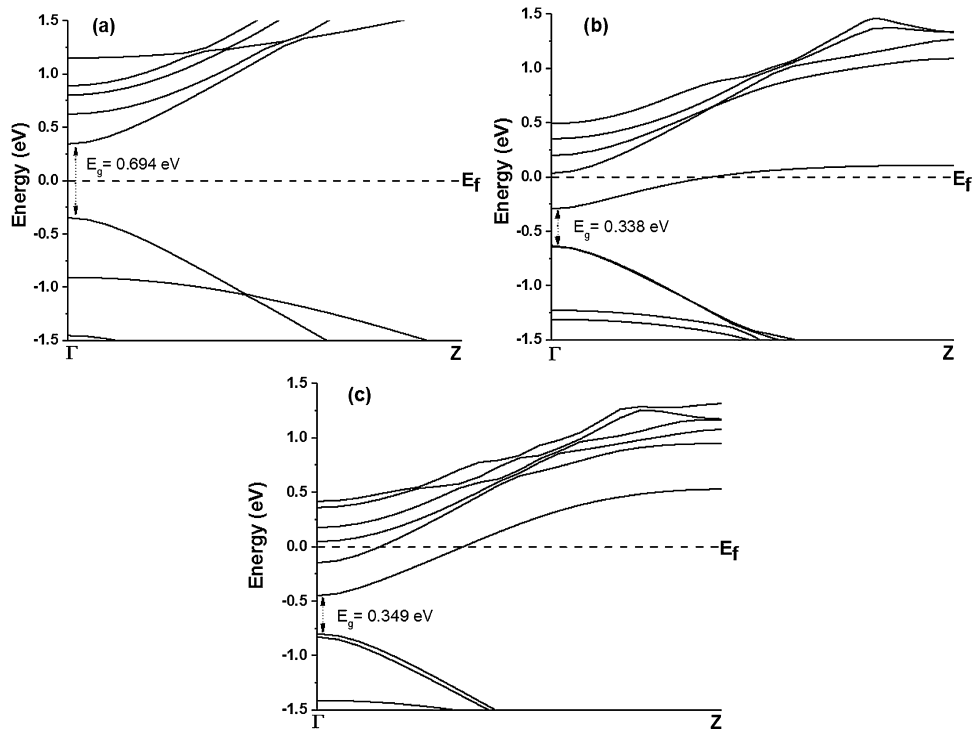


**Fig. 12.** The electronic band structure of the (a) pristine (10,0) SWCNT, (b) Cu-SWCNT and (c) H<sub>2</sub>S/Cu-SWCNT system. Fermi energy is shifted to the zero point.

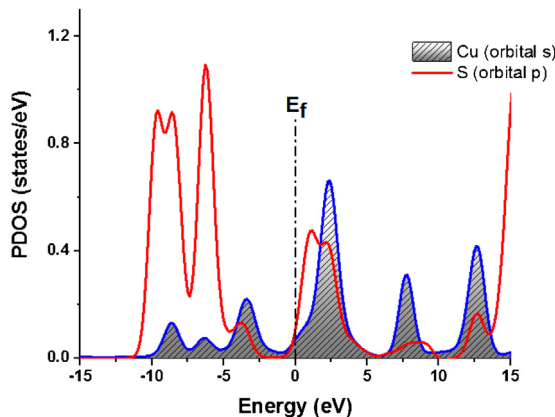


**Fig. 13.** The PDOS of Cu atom (3p-orbital) overlapped with S atom (4s-orbital) in the H<sub>2</sub>S/Cu-SWCNT system. The Fermi level is shifted to the zero point.

To understand the catalytic effects of the attached Cu atoms on the H<sub>2</sub>S adsorption, the partial-density-of-states (PDOS) due to the 3p-orbital of S and the 4s-orbital of Cu in H<sub>2</sub>S/Cu-SWCNT system are shown in Fig. 13. Due to the large overlap between the 3p and 4s orbitals, H<sub>2</sub>S is strongly hybridized with Cu. As a result, a SWCNT decorated with Cu NPs is an excellent candidate for H<sub>2</sub>S gas sensing.

#### 4. Conclusion

We have successfully demonstrated that Cu-SWCNTs-based sensors exhibit enhanced response upon exposure to various concentrations of H<sub>2</sub>S gas from 5 ppm to 150 ppm. A fast response time and a recovery time of 10 s and 15 s, respectively, have been achieved for 5 ppm of the target gas. The fabricated sensors show a high selectivity for 20 ppm H<sub>2</sub>S, whereas the concentrations of interfering gases were set to 200 ppm. The flexible sensors exhibit fast, stable, and reproducible responses at room temperature upon exposure to 20 ppm H<sub>2</sub>S. It is also found that the

resistance remains unchanged and the sensing performance is not considerably degraded over various bending radii for several times. In agreement with the experimental results, our theoretical analyses reveal that the Cu-SWCNT system strongly adsorbs H<sub>2</sub>S. The fabricated sensors can be used for real-time sensing of H<sub>2</sub>S with very high sensitivity and low power consumption that enable their integration with low power microelectronic circuits.

#### Acknowledgments

Authors acknowledge the technical discussion of the Prof. Mahdi Heidari Sani from Sharif University of Technology. Author would like to give special thanks to Mr. Hamed Farani from University of Tehran for Raman spectroscopy in preparing discussion section exhaustively.

#### References

- [1] Zh. Dai, L. Xu, G. Duan, T. Li, H. Zhang, Y. Li, Y. Wang, W. Cai, Fast-response, sensitivitive and low-powered chemosensors by fusing nanostructured porous thin film and IDEs-microheater chip, *Sci. Rep.* 3 (2012) 1669.
- [2] L. Valentini, I. Armentano, J.M. Kenny, C. Cantalini, L. Lozzi, S. Santucci, Sensors for sub-ppm NO<sub>2</sub> gas detection based on carbon nanotube thin films, *Appl. Phys. Lett.* 82 (2003) 961.
- [3] Sh. Nasrafahani, M.M. Doroodmand, M.H. Sheikhi, A.R. Ghasemi, Specific H<sub>2</sub>S gas sensor based on metal nanoparticles, sulfur and nitrogen/single-walled carbon nanotube-modified field effect transistor, *J. Nanoeng. Nanomanuf.* 1 (2011) 226–228.
- [4] M.K. Verma, V. Gupta, A highly sensitive SnO<sub>2</sub>–CuO multilayered sensor structure for detection of H<sub>2</sub>S gas, *Sens. Actuators B* 166 (2012) 378–385.
- [5] R.H. Zhang, X.T. Zhang, S.M. Hu, Novel sensor based on Ag/Ag<sub>2</sub>S electrode for in situ measurement of dissolved H<sub>2</sub>S in high temperature and pressure fluids, *Sens. Actuators B* 177 (2013) 163–171.
- [6] F. Shao, M.W.G. Hoffmann, J.D. Prades, R. Zamania, J. Arbiol, J.R. Morante, E. Varechkina, M. Rumyantseva, A. Gaskov, I. Giebelhaus, T. Fischer, S. Mathur, F. Hernández-Ramírez, Heterostructured p-CuO (nanoparticle)/n-SnO<sub>2</sub> (nanowire) devices for selective H<sub>2</sub>S detection, *Sens. Actuators B* 181 (2013) 130–135.
- [7] T.W. Odom, J. Huang, Ph. Kim, Ch.M. Lieber, Atomic structure and electronic properties of single-walled carbon nanotubes, *Nature* 391 (1998) 62–64.
- [8] T. Dürkop, S.A. Getty, E. Cobas, M.S. Fuhrer, extraordinary mobility in semiconducting carbon nanotubes, *Nano Lett.* 4 (2004) 35–39.

- [9] D.Y. Joh, J. Kinder, L.H. Herman, S. Ju, M.A. Segal, J.N. Johnson, G.K.-L. Chan, J. Park, Single-walled carbon nanotubes as excitonic optical wires, *Nat. Nanotechnol.* 6 (2011) 51–56.
- [10] C. Fantini, A. Jorio, M. Souza, M.S. Strano, M.S. Dresselhaus, M.A. Pimenta, Optical transition energies for carbon nanotubes from resonant Raman spectroscopy: environment and temperature effects, *Phys. Rev. Lett.* 93 (2004) 147406.
- [11] P.H. Lau, K. Takei, C. Wang, Y. Ju, J. Kim, Z. Yu, T. Takahashi, G. Cho, A. Javey, Fully-printed, high performance carbon nanotube thin-film transistors on flexible substrates, *Nano Lett.* 13 (8) (2013) 3864–3869.
- [12] Q. Cao, Sh. Han, G.S. Tulevski, Y. Zhu, D.D. Lu, W. Haensch, Arrays of single-walled carbon nanotubes with full surface coverage for high-performance electronics, *Nat. Nanotechnol.* 8 (2013) 180–186.
- [13] A. Javey, J. Guo, Q. Wang, M. Lundstrom, H. Dai, Ballistic carbon nanotube field-effect transistors, *Nature* 424 (2003) 654–657.
- [14] X. Chen, J. Zhu, Q. Xi, W. Yang, A high performance electrochemical sensor for acetaminophen based on single-walled carbon nanotube–graphene nanosheet hybrid films, *Sens. Actuators B* 161 (2012) 648–654.
- [15] P. Qi, O. Vermesh, M. Grecu, A. Javey, Q. Wang, H. Dai, Toward large arrays of multiplex functionalized carbon nanotube sensors for highly sensitive and selective molecular detection, *Nano Lett.* 3 (2003) 347–351.
- [16] Q. Zhao, Zh. Gan, Q. Zhuang, Electrochemical sensors based on carbon nanotubes, *Electroanalysis* 14 (2002) 1609–1613.
- [17] J. Wang, M. Musameh, Carbon nanotube/teflon composite electrochemical sensors and biosensors, *Anal. Chem.* 75 (2003) 2075–2079.
- [18] M. Asad, M.H. Sheikhi, Surface acoustic wave based  $H_2S$  gas sensors incorporating sensitive layers of single wall carbon nanotubes decorated with Cu nanoparticles, *Sens. Actuators B* 198 (2014) 134–141.
- [19] Z.K. Horastani, S.M. Sayedi, M.H. Sheikhi, Effect of single wall carbon nanotube additive on electrical conductivity and methane sensitivity of  $SnO_2$ , *Sens. Actuators B* 202 (2014) 461–468.
- [20] M. Penza, P. Aversaa, G. Cassanoa, W. Włodarskib, K. Kalantar-Zadeh, Layered SAW gas sensor with single-walled carbon nanotube-based nanocomposite coating, *Sens. Actuators B* 127 (2007) 168–178.
- [21] M. Yu, G. Suyambukasam, R. Wu, M. Chavali, Preparation of organic–inorganic (SWCNT/TWEEN–TEOS) nano hybrids and their NO gas sensing properties, *Sens. Actuators B* 161 (2012) 938–947.
- [22] J. Lee, W. Kang, Ch.Kh. Najeeb, B. Choi, S. Choib, H.J. Lee, S.S. Lee, J. Kim, A hydrogen gas sensor using single-walled carbon nanotube Langmuir–Blodgett films decorated with palladium nanoparticles, *Sens. Actuators B* 188 (2013) 169–175.
- [23] R.V. Sharma, N.K. Puri, R.K. Singh, A.M. Biradar, A. Mulchanadani, Label-free detection of cardiac troponin-I using gold nanoparticles functionalized single-walled carbon nanotubes based chemiresistive biosensor, *Appl. Phys. Lett.* 103 (2013) 203703.
- [24] B. Wang, J. Zheng, Y. He, Q. Sheng, A sandwich-type phenolic biosensor based on tyrosinase embedding into single-wall carbon nanotubes and polyaniline nanocomposites, *Sens. Actuators B* 186 (2013) 417–422.
- [25] M. Abdolahad, Sh. Mohajerzadeh, M. Jammaleki, H. Taghinejad, M. Taghinejad, Evaluation of the shear force of single cancer cells by vertically aligned carbon nanotubes suitable for metastasis diagnosis, *Integr. Biol.* 5 (2013) 535–542.
- [26] M. Abdolahad, M. Taghinejad, H. Taghinejad, M. Jammaleki, Sh. Mohajerzadeh, A vertically aligned carbon nanotube-based impedance sensing biosensor for rapid and high sensitive detection of cancer cells, *Lab Chip* 12 (2012) 1183–1190.
- [27] T. Ramanathan, H. Liu, L.C. Brinson, Functionalized SWNT/polymer nanocomposites for dramatic property improvement, *J. Polym. Sci. B: Polym. Phys.* 43 (2005) 2269–2279.
- [28] Y. Wang, Z. Iqbal, S.V. Malhotra, Functionalization of carbon nanotubes with amines and enzymes, *Chem. Phys. Lett.* 402 (2005) 69–101.
- [29] M. Penza, G. Cassano, R. Rossi, M. Alvisi, A. Rizzo, M.A. Signore, Th. Dikonomis, E. Serra, R. Giorgi, Enhancement of sensitivity in gas chemiresistors based on carbon nanotube surface functionalized with noble metal (Au, Pt) nanoclusters, *Appl. Phys. Lett.* 90 (2007) 173123.
- [30] D. Son, J. Lee, Sh. Qiao, R. Ghaffari, J. Kim, J.E. Lee, Ch. Song, S.J. Kim, D.J. Lee, S.W. Jun, Sh. Yang, M. Park, J. Shin, K. Do, M. Lee, K. Kang, Ch.S. Hwang, N. Lu, T. Hyeon, D. Kim, Multifunctional wearable devices for diagnosis and therapy of movement disorders, *Nat. Nanotechnol.* 9 (2014) 397–404.
- [31] K. Lee, V. Scardaci, H. Kim, T. Hallam, H. Nolan, B.E. Bolf, G.S. Maltbie, J.E. Abbott, G.S. Duesberg, Highly sensitive, transparent, and flexible gas sensors based on gold nanoparticle decorated carbon nanotubes, *Sens. Actuators B* 188 (2013) 571–575.
- [32] B. Hu, W. Chen, J. Zhou, High performance flexible sensor based on inorganic nanomaterials, *Sens. Actuators B* 176 (2013) 522–533.
- [33] V. Dua, S.P. Surwade, S. Ammu, S.R. Agnihotra, S. Jain, K.E. Roberts, S. Park, R.S. Ruoff, S.K. Manohar, All-organic vapor sensor using inkjet-printed reduced Graphene oxide, *Angew. Chem. Int. Ed.* 49 (2010) 2154–2157.
- [34] N. Saran, K. Parikh, D. Suh, E. Munoz, H. Kolla, S.K. Manohar, Fabrication and characterization of thin films of single-walled carbon nanotube bundles on flexible plastic substrates, *J. Am. Chem. Soc.* 126 (2004) 4462–4463.
- [35] A. Abdelhalim, A. Abdellah, G. Scarpa, P. Lugli, Fabrication of carbon nanotube thin films on flexible substrates by spray deposition and transfer printing, *Carbon* 61 (2013) 72–79.
- [36] Y. Wang, Z. Yang, Z. Hou, D. Xu, L. Wei, E.S. Kong, Y. Zhang, Flexible gas sensors with assembled carbon nanotube thin films for DMMP vapor detection, *Sens. Actuators B* 150 (2010) 708–714.
- [37] K. Parikh, K. Cattanach, R. Rao, D. Suh, A. Wu, S.K. Manohar, Flexible vapour sensors using single walled carbon nanotubes, *Sens. Actuators B* 113 (2006) 55–63.
- [38] K. Cattanach, R.D. Kulkarni, M. Kozlov, S.K. Manohar, Flexible carbon nanotube sensors for nerve agent simulants, *Nanotechnology* 17 (2006) 4123.
- [39] J. Pike, S. Chan, F. Zhang, X. Wang, J. Hanson, Formation of stable  $Cu_2O$  from reduction of  $CuO$  nanoparticles, *Appl. Catal. A* 303 (2006) 273–277.
- [40] J.M. Soler, E. Artacho, J.D. Gale, A. García, J. Junquera, P. Ordejón, D. Sánchez-Portal, The SIESTA method for ab-initio order-N materials simulation, *J. Phys.: Condens. Matter* 14 (2002) 2745–2779.
- [41] H.J. Monkhorst, J.D. Pack, Special points for Brillouin-zone integrations, *Phys. Rev. B* 13 (1976) 5188–5192.
- [42] M.S. Dresselhaus, G. Dresselhaus, A. Jorio, A.G.S. Filho, R. Saito, Raman spectroscopy on isolated single wall carbon nanotubes, *Carbon* 40 (2002) 2043–2061.
- [43] Z.H. Gan, G.Q. Yu, B.K. Tay, C.M. Tan, Z.W. Zhao, Y.Q. Fu, Preparation and characterization of copper oxide thin films deposited by filtered cathodic vacuum arc, *J. Phys. D: Appl. Phys.* 37 (2004) 81.
- [44] M. Yin, C. Wu, Y. Lou, C. Bruda, J.T. Koberstein, Y. Zhu, S. O'Brien, Copper oxide nanocrystals, *J. Am. Chem. Soc.* 127 (2005) 9506.
- [45] X. Zhang, Z. Dai, L. Wei, N. Liang, X. Wu, Theoretical calculation of the gas-sensing properties of Pt-decorated carbon nanotubes, *Sensors* 13 (2013) 15159–15171.
- [46] Z.K. Horastani, S.J. Hashemifar, S.M. Sayedi, M.H. Sheikhi, First-principles study of  $H_2$  adsorption on the pristine and oxidized (8, 0) carbon nanotube, *Int. J. Hydrogen Energy* 38 (2013) 13680–13686.
- [47] X. Kong, Y. Lee, High sensitivity of  $CuO$  modified  $SnO_2$  nanoribbons to  $H_2S$  at room temperature, *Sens. Actuators B* 105 (2005) 449–453.
- [48] M.S. Wagh, L.A. Patil, T. Seth, D.P. Amalnerkar, Surface cupricated  $SnO_2$ – $ZnO$  thick films as a  $H_2S$  gas sensor, *Mater. Chem. Phys.* 84 (2004) 228–233.
- [49] A. Chowdhuri, S.K. Singh, K. Sreenivas, V. Gupta, Contribution of adsorbed oxygen and interfacial space charge for enhanced response of  $SnO_2$  sensors having  $CuO$  catalyst for  $H_2S$  gas, *Sens. Actuators B* 145 (2010) 155–166.
- [50] V.R. Katti, A.K. Debnath, K.P. Muthe, M. Kaur, A.K. Dua, S.C. Gadkari, S.K. Gupta, V.C. Sahni, Mechanism of drifts in  $H_2S$  sensing properties of  $SnO_2$ : $CuO$  composite thin film sensors prepared by thermal evaporation, *Sens. Actuators B* 96 (2003) 245–252.
- [51] J.Y. Park, S.-W. Choi, J.W. Lee, C. Lee, S.S. Kim, Synthesis and gas sensing properties of  $TiO_2$ – $ZnO$  core–shell nanofibers, *J. Am. Ceram. Soc.* 92 (2009) 2551–2554.
- [52] A. Kolmakov, Y. Zhang, G. Cheng, M. Moskovits, Detection of  $CO$  and  $O_2$  using tin oxide nanowire sensors, *Adv. Mater.* 15 (2003) 997–1000.
- [53] Y.H. Lin, M.W. Huang, C.K. Liu, J.R. Chen, J.M. Wu, H.C. Shih, The preparation and high photon-sensing properties of fluorinated tin dioxide nanowires, *J. Electrochem. Soc.* 156 (2009) K196–K199.

## Biographies

**Mohsen Asad** is a PhD candidate and research assistant at Semiconductor Device Research Center, School of Electrical and Computer Engineering, Shiraz University, Iran. He has published over 17 articles in journals and conference papers and hold four patents in the field of chemical sensors. His research interests include fabrication of prototype devices based on quantum and semiconductor science considering functional materials (1D and 2D based systems) in chemical and biological sensors.

**Mohammad Hossein Sheikhi** received his BSc (1994) degree in electrical engineering from Shiraz University, Shiraz, Iran, the MSc (1996) degree from Sharif University of Technology, Tehran, Iran and the PhD degree in electrical engineering from Tarbiat Modares University, Tehran in 2000. He was selected as the distinguished PhD student graduated from Tarbiat Modares University in 2000. He joined Tohoku University, Sendai, Japan, as a Research Scientist in 2000. After joining Shiraz University in 2001, he focused on the optoelectronics, nanosensors, and nanotransistors. He is currently the Associate Professor and founder of Semiconductor Device Research Center, Shiraz University, Shiraz, Iran.

**Mahdi Pourfath** was born in Tehran, Iran, in 1978. He received the BS and MS degrees in electrical engineering from Sharif University of Technology, Tehran, in 2000 and 2002, respectively, and the PhD degree in Microelectronics from the Technische Universität Wien, Austria, in 2007. He has authored or co-authored over 100 scientific publications and presentations and authored one monograph. He is now an Assistant Professor in the School of Electrical and Computer Engineering, University of Tehran. He is also with the Institute of Microelectronics, Technische Universität Wien, Austria. His scientific interests include novel nanoelectronic devices and materials.

**Mahmood Moradi** received his BSc degree (1977) in Physics from Isfahan University, the MSc (1981) from Shiraz University and the PhD (1989) in condensed matter Physics from Kent University in England. Now he is professor in Physics Department in Shiraz University and working on density functional theory, nanostructures, spintronics and liquid crystals. He has published more than 55 papers in international journals and held more than 100 presentations in national and international conferences.